Dyskinesis in chagasic myocardium: centerline analysis of wall motion using cardiac-gated magnetic resonance images of mice[★]

Jorge L. Durand[a], **Baiyu Tang**[a], **David E. Gutstein**[d], **Stefka Petkova**[b], **Mauro M. Teixeira**[e], **Herbert B. Tanowitz**[b,c], and **Linda A. Jelicks**[a,*]

a*Department of Physiology and Biophysics, Albert Einstein College of Medicine, Bronx, NY 10461, USA*

b*Department of Pathology, Albert Einstein College of Medicine, Bronx, NY 10461, USA*

c*Division of Infectious Disease, Department of Medicine, Albert Einstein College of Medicine and Montefiore Medical Center, Bronx, NY 10461, USA*

d*Departments of Medicine (Cardiology) and Cell Biology, New York University School of Medicine, New York, NY 10016, USA*

e*Departamento de Bioquimica e Imunologia, Instituto de Ciencias Biologicas, Universidade Federal de Minas Gerais, 31270−901 Belo Horizonte MG, Brazil*

Abstract

We report on the use of centerline analysis of cardiac-gated magnetic resonance images to measure wall motion abnormalities in mice infected with *Trypanosoma cruzi*. To our knowledge, this is the first report of segmental wall motion abnormalities in an animal model of Chagas' disease. Chagas' disease patients with severe cardiac involvement exhibit mild hypokinesis in an extensive region of the left ventricle and dyskinesis in the apical region. We observed dyskinetic segments in a similar region of the hearts of infected wild-type mice. Dyskinesis was not observed in infected mice lacking macrophage inflammatory protein-1α, a chemokine that may play an important role in the cardiac remodeling that is normally observed in mouse models of Chagas' disease and in human patients. This study aimed to demonstrate the utility of cardiac-gated magnetic resonance imaging and centerline analysis as a straightforward method for monitoring regional left ventricular wall motion in transgenic and/or diseased mice.

Keywords

Magnetic resonance imaging; Left ventricle; Centerline; Wall motion; Cardiac gated; Mice

1. Introduction

Magnetic resonance imaging (MRI) has become the gold standard for assessing human cardiac anatomy and function. In the murine, cardiac imaging conditions are more challenging due to the small size and rapid rate of the mouse heart; nevertheless, techniques such as FLASH and spin-echo imaging have been shown to be very useful. Many novel mouse models of cardiovascular disease exhibit myocardial dysfunction at the cellular and tissue levels—in

particular, mouse models of Chagas' disease and myocardial infarction may exhibit regional wall motion abnormalities; therefore, methods that can evaluate regional function in mouse models are very important. Anatomical MRI, echocardiography and ECG are valuable for assessing global myocardial function but may not detect regional abnormalities; tagged cine-MRI can be used to evaluate regional function and has been applied to noninvasively measure left ventricular (LV) torsion in mice [1]. The contraction of the helical ventricular fibers results in a twisting motion of the left ventricle about its axis and has been shown to be equivalent in humans and mice [1].In humans, segmental analysis of echocardiography-derived color kinesis images has been correlated with angiography results and was demonstrated to be more sensitive, specific and accurate than the subjective reading of conventional echocardiograms for the assessment of regional LV and RV function. This method is a promising, simple and fast technique for assessing myocardial risk in humans [2,3]. Significant progress has been made in the study of mouse LV morphology and function using echocardiography and MRI despite technical challenges. Echocardiographic evaluation of mouse ventricular function and chamber volumes after induction of myocardial infarction has been applied in combination with visual wall motion analysis and has been shown to be useful for assessing both chronic and acute responses to ischemia in a variety of mouse models [4]. While echocardiography is valuable for assessing global function in mice, MRI can provide three-dimensional views of the heart that facilitate evaluation of regional function and segmental wall motion abnormalities.

Centerline analysis has been previously applied in cardiac imaging studies on LV wall thickness in humans and animals [5-10]. We recently developed a robust algorithm for centerline analysis of MR images and applied the method to measure right ventricular (RV) wall thickness in mice [11]. In the present report, we applied centerline analysis of diastolic and systolic MR images of the long axis of the heart to study regional wall motion in mice that were infected with *Trypanosoma cruzi*. Infection with the protozoan parasite *T. cruzi* causes Chagas' disease, a disease that affects nearly 20 million people in Central and South America and results in approximately 50,000 deaths each year [12]. Chagas' disease is first manifested by a short acute phase characterized by the presence of parasites in the bloodstream. This is followed by a lifelong chronic phase characterized by scarce parasitemia. Many infected individuals remain free of symptoms, but 10−30% of patients will ultimately develop defined clinical syndromes, including chronic myocarditis, cardiomegaly, congestive heart failure, arrhythmias and destruction of skeletal muscles and/or the digestive tract. Mice infected with *T. cruzi* develop progressive chronic cardiomyopathy similar to that observed in humans [13-16].

CCL3/macrophage inflammatory protein-1α (MIP-1α)is a chemokine whose receptor has been implicated in the pathogenesis of chagasic heart disease [17] and is essential for the host to deal with acute infection [18,19]. It was also shown that pharmacological blockade of the chemokine receptor, CCR5, prevents chronic inflammation in *T. cruzi*-infected mice [20]. These studies suggest that the absence of chemokines such as MIP-1α may prevent inflammation during acute and chronic experimental *T. cruzi* infections and thus limit the cardiac remodeling that is typically observed in infected mice [13-16].

We report on regional wall motion abnormalities in mice infected with *T. cruzi* and demonstrate the feasibility of using MRI and a centerline approach to evaluate regional wall motion in mouse models of human disease.

2. Materials and methods

2.1. Animals

Male MIP-1α null and C57BL/6×129sv control mice (Jackson Laboratory, Bar Harbor, ME, USA) were housed in our institution. Mice were infected intraperitoneally with $5×10^4$ trypomastigotes of the Brazil strain of *T. cruzi*. Parasitemia was determined by counting parasites in a hemocytometer chamber and was not significantly different between infected groups. All animal protocols were approved by our institutional animal care and use committee.

2.2. MRI

At 120 days postinfection, mice were injected intraperitoneally with ketamine (37.5−75 mg/kg) and xylazine (7−14 mg/kg) anesthesia. Once mice were anesthetized, ECG cables (Gould Instruments, OH, USA) with thin silver wire contacts were attached under the skin to the four limbs. ECG SNR was improved by maximizing skin contact with the wire and by using a thin Teflon sheet that covers the mice and minimizes contact of the ECG leads with the RF coil. A NESLAB gradient water cooling system, set to maintain the temperature inside the coil at 30 °C, was used to prevent hypothermia. Acquisition of several multislice imaging data sets at different time points of the cardiac cycle during a 30- to 45-min period of anesthesia was possible under these conditions. Cardiac-gated MRI was performed as described in previous work [11,13-15]. A GE Omega 9.4-T vertical bore MR system (Fremont, CA, USA) with a gradient strength of 75 G/cm provided by an S50 shielded gradient microimaging accessory and a homebuilt 35-mm-inner diameter linear cosine litz coil constructed specifically for mice [11,21] were used for the MRI experiments. Cosine coils of this kind require few capacitors for frequency tuning, are easy to construct and can achieve high-field homogeneity [22]. Importing the litz coil design permits current to flow more equally through each leg of the coil [23]. Diastolic and systolic images were acquired by adjusting the spectrometer gating delay according to the heart rate determined from the ECG. An echo time of 18 ms and a repetition time of approximately 100−200 ms were the parameters used in several multislice spin-echo scout imaging data sets of the short axis of the heart. We positioned the long-axis images to approximate the right anterior oblique projections used in human ventriculogram studies as shown in the work of Sheehan et al. [7] and in Fig. 1. A 40-mm field of view (FOV) was used for short-axis images and a 60-mm FOV was used for long-axis images, with a 128×256 matrix size (interpolated to 256×256) in both cases. A series of images of the heart were acquired at various time points in the cardiac cycle by stepping through the RR interval in 20-mm increments. The end-diastolic data set (exhibiting the largest LV inner chamber diameter) and end-systolic data set (exhibiting the smallest LV inner chamber diameter) were selected for analysis. MATLAB-based custom-designed software was used for analysis of MRI data. Long-axis images of the heart were registered using anatomical landmarks (mitral valve).

2.3. Centerline analysis of regional wall motion

The centerline method has been improved and applied to regional LV function analysis [5-10,24,25]. As previously reported, we developed a robust algorithm for centerline analysis and applied it to study mouse heart wall thickness [11,26]. The centerline is the curve midway between two contours on heart images. The length distribution of the chords that are perpendicular to the centerline and that start at one contour and end at the other contour quantifies the local distance between two contours. The Fourier descriptor [27] is applied to express the borders and centerline. The curves and chords are parameterized using Fourier series. In our previous study, we applied this approach using the open-border method to measure the mouse heart RV wall thickness [11,25]. Here, we used this method for measurement of regional wall motion in mice infected with *T. cruzi*. In this study, using end-systolic and end-diastolic images of the heart, the distance between the two contours is interpreted as regional wall motion. After the centerline of the end-systolic and end-diastolic

LV walls was calculated, the wall motion was plotted as a function of region (see Fig. 1). Regional wall motion was evaluated in a distribution of 100 chords along the ventricular walls. A more detailed description of the steps and all operations applied in our algorithm can be found in a recent article from our group [11].

2.4. Statistics

All results were analyzed using a one-sided unpaired *t* test. A *P* value of <.05 was deemed significant.

3. Results

Three uninfected MIP-1α null mice, four uninfected C57BL/6×129sv mice, three infected MIP-1α null mice and three infected C57BL/6×129sv mice were examined by MRI. Several multislice scout data sets consisting of four to eight images of the short axis of the heart were acquired and used to determine positioning of the long-axis images of the left ventricle. Short-axis images of the heart were used to evaluate LV wall thickness and chamber dimensions during diastole and systole. Representative short-axis diastolic images are shown in Fig. 2.

There was no significant difference in the LV wall thickness or LV chamber dimension between the four groups of mice (Table 1). Fractional shortening was calculated using the LV inner diameters determined from the diastole and systole short-axis images of the heart at mid-ventricle and was not different between groups. Short-axis images were chosen for analysis of fractional shortening for comparison with previous echocardiography and MRI studies from our lab. Fractional shortening was 56.7±6.1% in uninfected MIP-1α null mice, was 58±3.5% in uninfected C57BL/6×129sv mice, was 59.3±2.4% in infected MIP-1α null mice and was 57.7±4.3% in infected C57BL/6×129sv mice.

Representative long-axis images of the heart of a mouse during end systole and end diastole are shown in Fig. 3. Regional wall motion analysis results for one mouse from each group are shown in Fig. 4 for the area of interest, Chords 25 to 75, which cover the apical and diaphragmatic regions. Fig. 5 shows the regional analysis results for all the different groups. As expected, there was no evidence of dyskinesis in the LV wall of the uninfected wild-type C57BL/6×129sv mice. There was also no region of dyskinesis in any region of the wall of the MIP-1α null mice whether they were infected with the parasite or not. In contrast, the infected C57BL/6×129sv mice exhibited dyskinesis in the apical–diaphragmatic region.

4. Discussion

As predicted based on our previous studies [13-16], the RV chamber of infected C57BL/6×129sv mice exhibited significant dilatation as compared with uninfected C57BL/×6 129sv mice [see RV inner diameter (RVID) in Table 1]. There was no significant difference in the RVID between infected and uninfected MIP-1α null mice. This result supports the hypothesis that the absence of chemokines such as MIP-1α prevents inflammation and limits the cardiac remodeling that is typically observed in infected mice [13-16]. Although fractional shortening was not significantly different in the infected C57BL/6×129sv mice, these mice had abnormal wall motion, primarily in the apical region (as described in more detail below).

MIP-1α is a chemokine expressed in response to *T. cruzi* infection of macrophages and in vivo [18,19] and acts on CCR5, a chemokine receptor known to be essential for the ability of the host to deal with the acute infection [17]. It has been shown that pharmacological blockade of CCR5 prevents chronic inflammation in *T. cruzi*-infected mice [20]. These studies suggest that the absence of chemokines such as MIP-1α may limit inflammation during acute and chronic experimental *T. cruzi* infections and thus reduce the cardiac remodeling that is typically

observed in infected mice. In fact, histopathological examination of the hearts revealed that there was inflammation but no fibrosis in MIP-1α null hearts after 4 months of infection. However, in infected wild-type hearts, there was significant fibrosis.

It is interesting to note that, although fractional shortening was not different, the C57BL/6×129sv mice infected with *T. cruzi* exhibited dyskinesis in the apical–diaphragmatic region of the LV wall. This finding highlights the importance of evaluating regional function as opposed to relying on methods that report on global function. In a study on 14 patients with chronic Chagas' disease accompanied by abnormal wall motion, 10 patients exhibited dyskinesis, 3 exhibited apical akinesis, 9 exhibited akinesis or hypokinesis of the posteroinferior wall, 4 exhibited akinesis and 2 exhibited hypokinesis of the posterior septum [28]. Of the 10 patients with apical wall motion abnormalities, 3 had normal ECGs, again highlighting the importance of evaluating regional function [28]. In a different study, 85% of patients with mild ventricular dilation and normal LV function exhibited mild hypokinesis, while all patients with more severe cardiac disease exhibited abnormally contracting segments [29].

Since myocardial wall motion abnormalities in chagasic cardiomyopathy tend to be focal and in the majority of patients localize to the apical or periapical segments [30,31], we decided to study LV wall motion using long-axis images of the heart. The focal areas of myocardial dysfunction in Chagas' disease patients are associated with abnormal myocardial perfusion as detected by thallium imaging, although they are not associated with epicardial coronary disease [32]. In Chagas' disease patients who have minor wall motion abnormalities detected by echocardiography, estimates of global LV function using short-axis measurements underestimate the extent of overall dysfunction [33]. One reason for the underestimation of ventricular dysfunction in Chagas' cardiomyopathy using short-axis measurements is that the short-axis view excludes the apex and periapical segments. It is for this reason that we elected to use the long-axis view for the centerline analysis in our murine model of Chagas' cardiomyopathy. The long-axis view allows for a direct comparison of regional wall motion between the apical and basal segments of the heart in a single two-dimensional image.

5. Conclusions

Our previous MRI and echocardiographic studies on wild-type mice infected with *T. cruzi* demonstrated evidence of remodeling of the right ventricle and abnormalities in fractional shortening [14-17,34]; however, this is the first report of LV wall motion abnormalities in a mouse model of Chagas' disease.

Application of the centerline method for LV wall motion analysis from MRI data of mice is easy to implement and provides rapid reproducible results. We previously demonstrated the utility of the method for RV wall thickness analysis in mice. This approach allows us to analyze results from studies performed in a high-field vertical bore magnet (9.4 T) with animal models of infectious disease, such as Chagas' disease. This method permits a high throughput, which is important for serial studies in which we have a larger cohort of mice that are diseased and may not survive the longer preparation and acquisition times required for more sophisticated tagging experiments.

Acknowledgments

References

1. Henson RE, Song SK, Pastorek JS, Ackerman JJH, Lorenz CH. Left ventricular torsion is equal in mice and humans. Am J Physiol 1999;278:H1117–23.

2. Vignon P, Weinert L, Mor-Avi V, Spencer KT, Bednarz J, Lang RM. Quantitative assessment of regional right ventricular function with color kinesis. Am J Respir Crit Care Med 1999;159:1949–59. [PubMed: 10351944]

3. Koch R, Lang RM, Garcia MJ, Weinert L, Bednarz J, Korcarz C, et al. Objective evaluation of regional left ventricular wall motion during dobutamine stress echocardiographic studies using segmental analysis of color kinesis images. J Am Coll Cardiol 1999;34:409–19. [PubMed: 10440153]

4. Scherrer-Crosbie M, Steudel W, Hunziker PR, Liel-Cohen N, Ullrich WM, Zapol WM, et al. Three-dimensional echocardiographic assessment of left ventricular wall motion abnormalities in mouse myocardial infarction. J Am Soc Echocardiogr 1999;12:834–40. [PubMed: 10511652]

5. Hubka M, Lipiecki J, Bolson EL, Martin RW, Munt B, Maza SR, et al. Three-dimensional echocardiographic measurement of left ventricular wall thickness: in vitro and in vivo validation. J Am Soc Echocardiogr 2002;15:129–35. [PubMed: 11836487]

6. Sheehan FH, Schofer J, Mathey DG, Kellett MA, Smith H, Bolson EL, et al. Measurement of regional wall motion from biplane contrast ventriculograms: a comparison of the 30 degree right anterior oblique and 60 degree left anterior oblique projections in patients with acute myocardial infarction. Circulation 1986;74:796–804. [PubMed: 3757191]

7. Sheehan FH, Bolson EL, Dodge HT, Mathey DG, Schofer J, Woo HW. Advantages and applications of the centerline method for characterizing regional ventricular function. Circulation 1986;74:293–305. [PubMed: 3731420]

8. Buller VG, van der Geest RJ, Kool MD, van der Wall EE, de Roos A, Reiber JH. Assessment of regional left ventricular wall parameters from short axis magnetic resonance imaging using a three-dimensional extension to the improved centerline method. Invest Radiol 1997;32:529–39. [PubMed: 9291041]

9. Holman ER, Buller VG, de Roos A, van der Geest RJ, Baur LH, van der Laarse A, et al. Detection and quantification of dysfunctional myocardium by magnetic resonance imaging. A new three-dimensional method for quantitative wall-thickening analysis. Circulation 1997;95:924–31. [PubMed: 9054752]

10. Holman ER, Vliegen HW, van der Geest RJ, Reiber JH, van Dijkman PR, van der Laarse A, et al. Quantitative analysis of regional left ventricular function after myocardial infarction in the pig assessed with cine magnetic resonance imaging. Magn Reson Med 1995;34:161–9. [PubMed: 7476074]

11. De Souza AP, Cohen AW, Park DS, Woodman SE, Tang B, Gutstein DE, et al. MR imaging of caveolin gene-specific alterations in right ventricular wall thickness. Magn Reson Imaging 2005;23:61–68. [PubMed: 15733789]

12. WHO. Tropical Disease Research, Thirteenth Program Report. UNDP/WB/TDR; Geneva: 1997. Chagas' disease..

13. Jelicks LA, Shirani J, Wittner M, Chandra M, Weiss LM, Factor SM, et al. Application of cardiac gated magnetic resonance imaging in murine Chagas' disease. Am J Trop Med Hyg 1999;61:207–14. [PubMed: 10463668]

14. Huang H, Chan J, Wittner M, Jelicks LA, Morris SA, Factor SM, et al. Expression of cardiac cytokines and inducible form of nitric oxide synthase (NOS2) in Trypanosoma cruzi-infected mice. J Mol Cell Cardiol 1999;31:75–88. [PubMed: 10072717]

15. Jelicks LA, Chandra M, Shirani J, Shtutin V, Tang B, Christ CJ, et al. Cardioprotective effects of phosphoramidon on myocardial structure and function in murine Chagas' disease. Int J Parasitol 2002;32:1497–506. [PubMed: 12392915]

16. Chandra M, Shirani J, Shtutin V, Weiss LM, Factor SM, Petkova SB, et al. Cardioprotective effects of verapamil on myocardial structure and function in a murine model of chronic Trypanosoma cruzi infection (Brazil strain): an echocardiographic study. Int J Parasitol 2002;32:207–15. [PubMed: 11812498]

17. Machado FS, Koyama NS, Carregaro V, Ferreira BR, Milanezi CM, Teixeira MM, et al. CCR5 plays a critical role in the development of myocarditis and host protection in mice infected with Trypanosoma cruzi. J Infect Dis 2005;11:627–36. [PubMed: 15655788]

18. Aliberti JC, Machado FS, Souto JT, Campanelli AP, Teixeira MM, Gazzinelli RT, et al. beta-Chemokines enhance parasite uptake and promote nitric oxide-dependent microbiostatic activity in murine inflammatory macrophages infected with Trypanosoma cruzi. Infect Immun 1999;67:4819–26. [PubMed: 10456936]

19. Talvani A, Ribeiro CS, Aliberti JC, Michailowsky V, Santos PV, Murta SM, et al. Kinetics of cytokine gene expression in experimental chagasic cardiomyopathy: tissue parasitism and endogenous IFN-gamma as important determinants of chemokine mRNA expression during infection with Trypanosoma cruzi. Microbes Infect 2000;2:851–66. [PubMed: 10962268]

20. Marino AP, da Silva A, dos Santos P, Pinto LM, Gazzinelli RT, Teixeira MM, et al. Regulated on activation, normal T cell expressed and secreted (RANTES) antagonist (Met-RANTES) controls the early phase of Trypanosoma cruzi-elicited myocarditis. Circulation 2004;110:1341–2. [PubMed: 15364818]

21. Tang, B.; Jelicks, LA. Book of abstracts: Eleventh Annual Meeting of the Society of Magnetic Resonance in Medicine. Vol. 10. ISMRM; Berkeley (Calif): 2002. Two placements of cosine coil legs.; p. 876

22. Bolinger L, Prammer MG, Leigh JS Jr. A multiple-frequency coil with a highly uniform B1 field. J Magn Reson 1988;81:162–6.

23. Doty DF, Entzminger G Jr, Hauck CD. Error-tolerant RF litz coils for NMR/MRI. J Magn Reson 1999;140:17–31. [PubMed: 10479546]

24. von Land, CD.; Rao, SR.; Reiber, JHC. Computers in cardiology. IEEE Computer Society Press; 1990. Development of an improved centerline wall motion model.; p. 687-90.

25. Wilson, MD. Visualization and presentation of CAMRA data sets and results of semi-automatic segmentation of cardiac MR images (Report) EPCC-SS99−02 Extension to CAMRA. EPCC University of Edinburgh; UK: 2000. p. 4-14.

26. Tang, B.; Jelicks, LA.; Gutstein, DE. Book of abstracts: Eleventh Annual Meeting of the Society of Magnetic Resonance in Medicine. Vol. 10. ISMRM; Berkeley (CA): 2002. A robust algorithm of centerline for heart image analysis.; p. 2464

27. Staib LH, Duncan JS. Boundary finding with parametrically deformable models. IEEE Trans Pattern Anal Mach Intell 1992;14:1061–75.

28. Acquatella H, Pérez JE, Condado JA, Sánchez I. Limited myocardial contractile reserve and chronotropic incompetence in patients with chronic Chagas' disease. J Am Col Cardiol 1999;33:522–9.

29. Simões MV, Pintya AO, Bromberg-Marin G, Sarabanda AV, Marques Antloga C, Pazin-Filho A, et al. Relation of regional sympathetic denervation and myocardial perfusion disturbance to wall motion impairment in Chagas' cardiomyopathy. Am J Cardiol 2000;86:975–81. [PubMed: 11053710]

30. Hammermeister KE, Caeiro T, Crespo E, Palmero H, Gibson DG. Left ventricular wall motion in patients with Chagas's disease. Br Heart J 1984;51(1):70–6. [PubMed: 6689924]

31. Maciel BC, Almeida-Filho OC, Schmidt A, Marin-Neto JA. Ventricular function in Chagas' heart disease. São Paulo Med J 1995;113:814–20.

32. Marin-Neto JA, Marzullo P, Marcassa C, Gallo Junior L, Maciel BC, Bellina CR, et al. Myocardial perfusion abnormalities in chronic Chagas' disease as detected by thallium-201 scintigraphy. Am J Cardiol 1992;69(8):780–4. [PubMed: 1546653]

33. de Almeida-Filho OC, Maciel BC, Schmidt A, Pazin-Filho A, Marin-Neto JA. Minor segmental dyssynergy reflects extensive myocardial damage and global left ventricle dysfunction in chronic Chagas disease. J Am Soc Echocardiogr 2002;15(6):610–6. [PubMed: 12050602]

34. Tanowitz HB, Huang H, Jelicks LA, Chandra M, Loredo ML, Weiss LM, et al. Role of endothelin 1 in the pathogenesis of chronic chagasic heart disease. Infect Immun 2005;73:2496–503. [PubMed: 15784596]
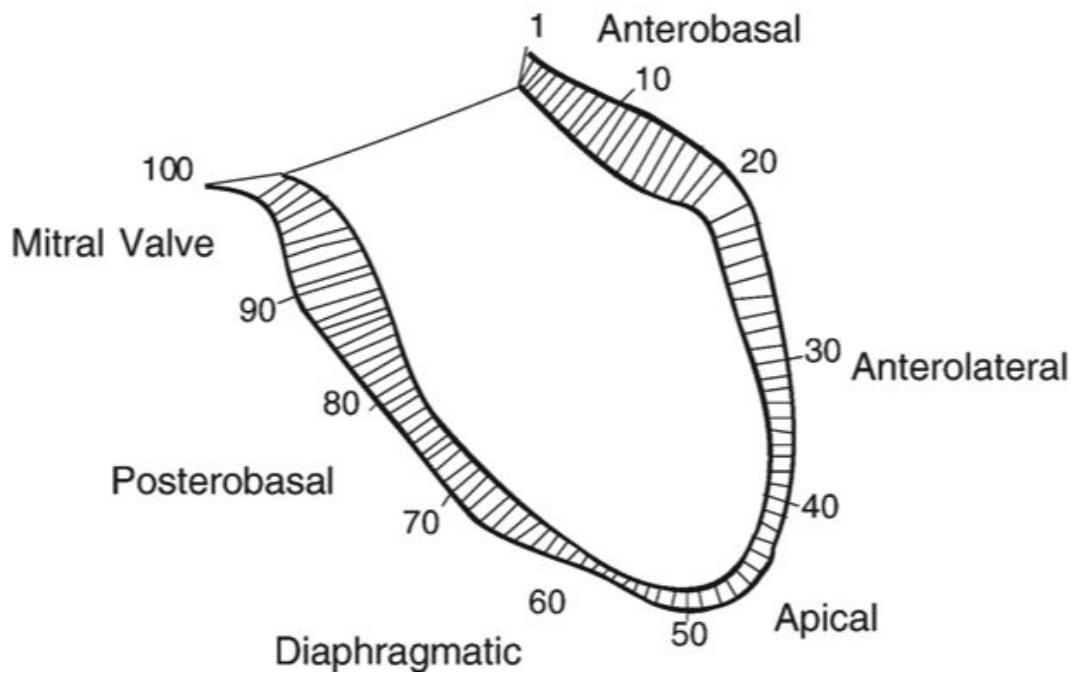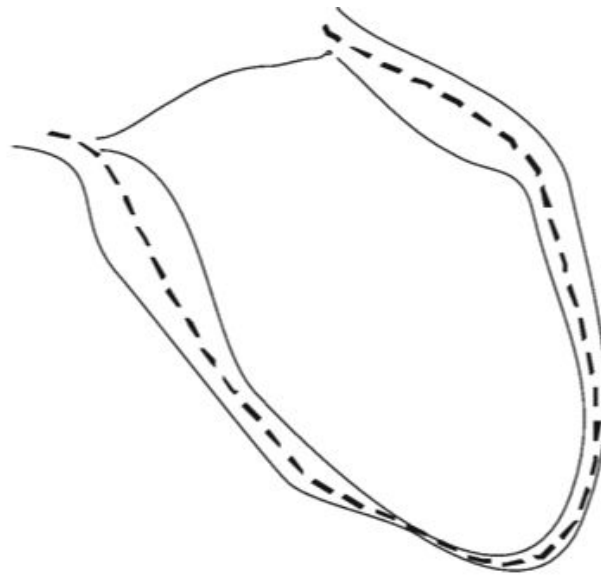
Fig. 1.
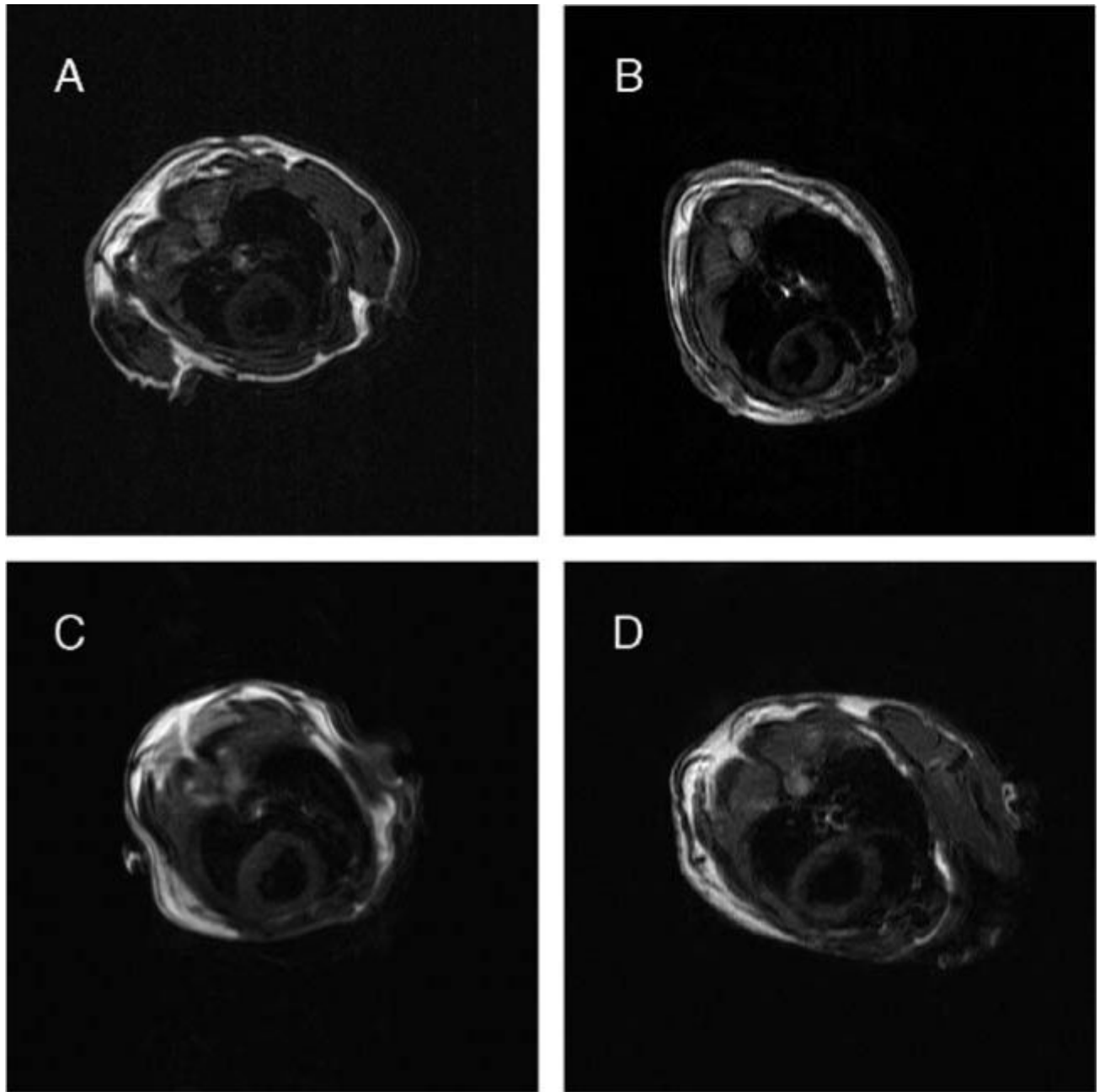Schematic diagram showing the distribution of chords along the walls of the left ventricle of the heart.

Fig. 2.
Representative short-axis diastolic spin-echo MR images of mice. A: uninfected MIP-1α null;
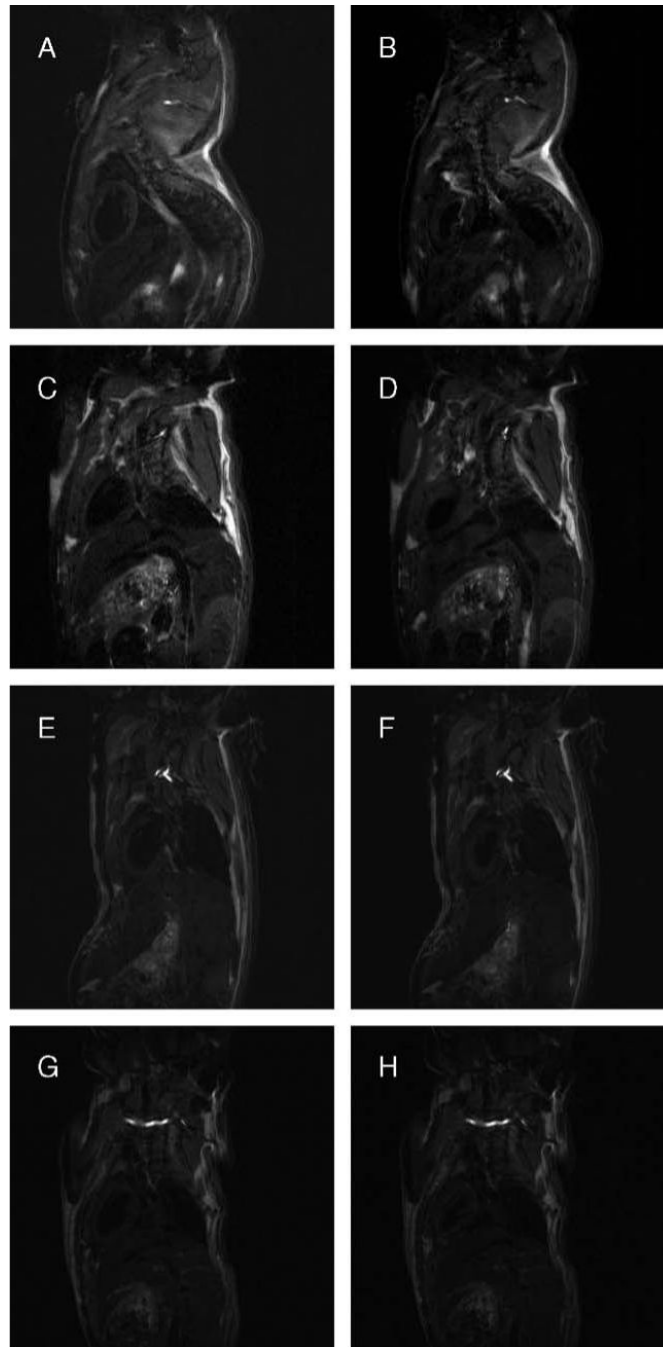B: infected MIP-1α null; C: uninfected C57BL/6×129sv; D: infected C57BL/6×129sv.

Fig. 3.
Representative long-axis systolic and diastolic MR images of mice. Representative long-axis spin-echo images of the hearts of mice (A and B: uninfected C57BL/6×129sv; C and D: infected C57BL/6×129sv; E and F: uninfected MIP-1α null; G and H: infected MIP-1α null) at end diastole (panels on left) and end systole (panels on right) as used for centerline analysis.

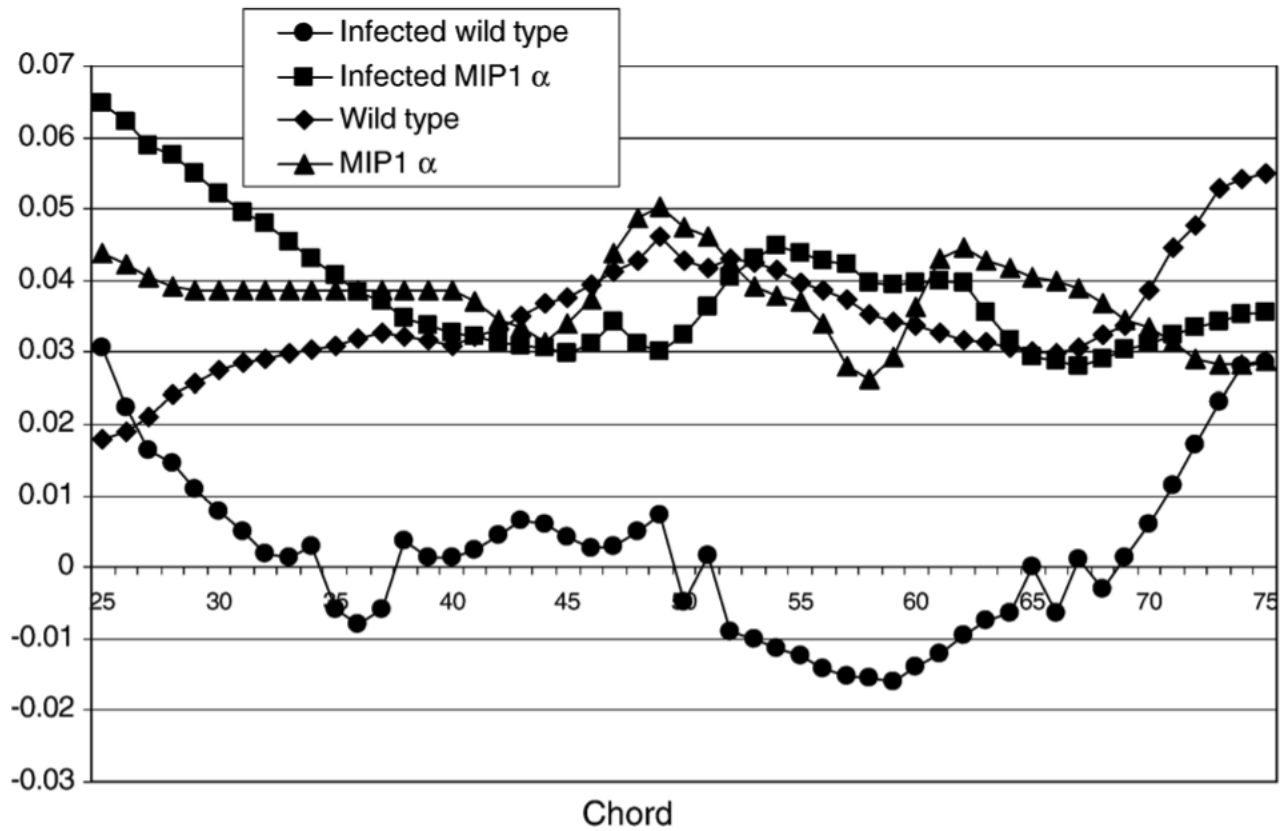## Normalized Wall Motion By Chord Number

Fig. 4.
Plot of wall motion versus chord number for one representative mouse from each group. For clarity of presentation, results from one mouse from each group are shown for Chords 25−75, which encompass the apical and diaphragmatic regions.
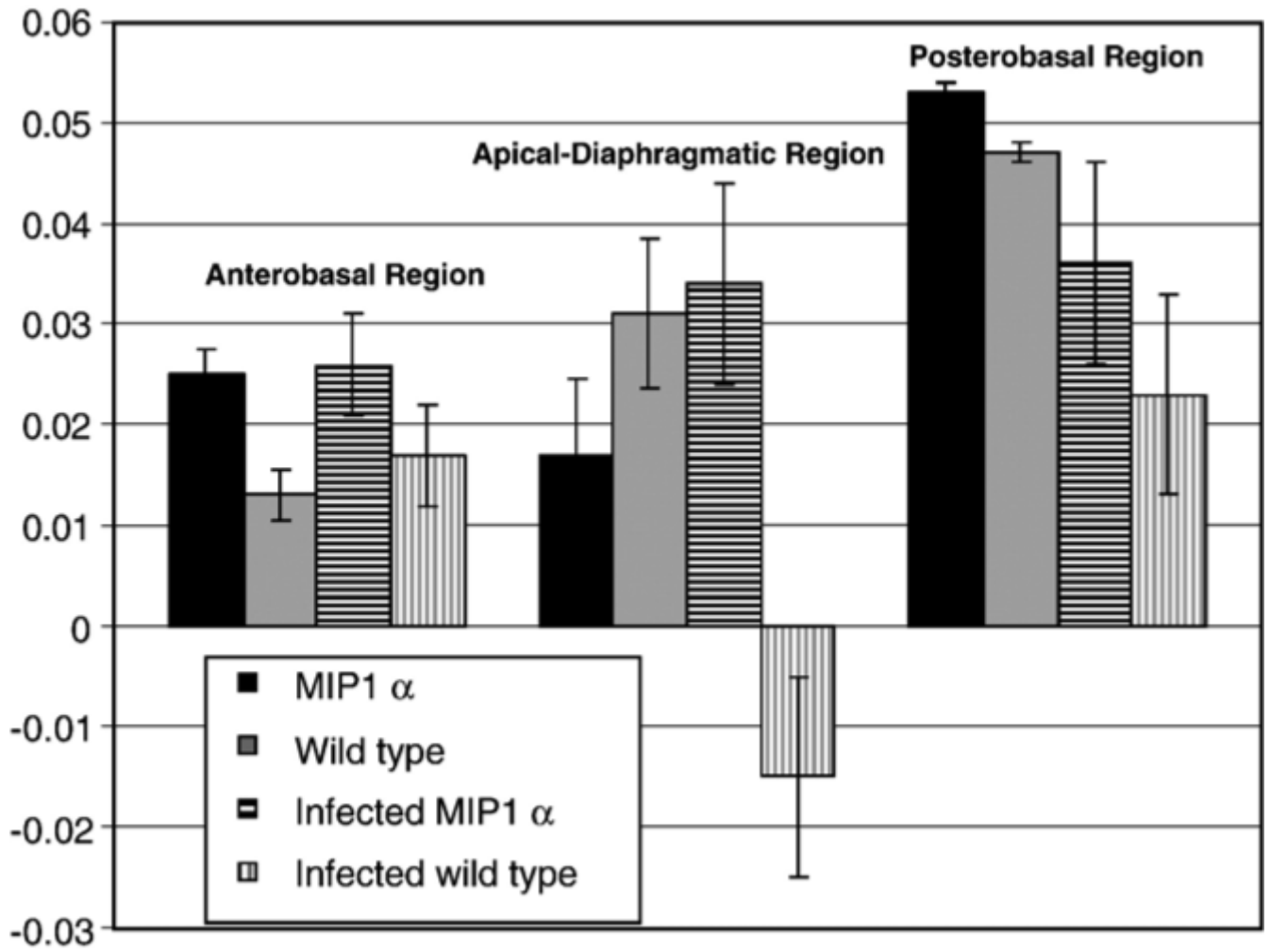
Fig. 5.
Normalized wall motion by region. Bar graph (mean±S.E.M.) of normalized wall motion by heart region for the four groups of mice showing the dyskinesis in the infected wild-type mice in the apical–diaphragmatic region.

Table 1

End-diastolic LV and RV inner chamber dimensions and LV wall thickness determined from cardiac-gated short-axis images of the heart

Mouse strain	n	LVID (mm)	LV wall thickness[a] (mm)	RVID (mm)
Uninfected MIP-1α null	3	3.21±0.28	1.15±0.13	1.83±0.25
Uninfected C57BL/6×129sv	4	3.94±0.16	1.07±0.09	1.93±0.3
Infected MIP-1α	3	3.45±0.15	1.08±0.09	1.73±0.15
Infected C57BL/6×129sv	3	3.81±0.24	1.12±0.03	2.70±0.26[b]

Data are expressed as mean±S.E.M. LVID indicates LV inner diameter.

[a] The average of the septal, anterior, posterior and lateral walls.

[b] RVID was significantly larger in infected C57BL/6×129sv mice as compared with the other groups of mice ($P<.05$). LVID tended to be smaller in MIP-1α null mice regardless of infection. LV wall thickness was not different between groups.